HHS Public Access

Author manuscript

J Immunol. Author manuscript; available in PMC 2022 December 15.

Published in final edited form as:

J Immunol. 2021 December 15; 207(12): 2944–2951. doi:10.4049/jimmunol.2100650.

H2-O does not preempt autoimmunity but controls murine γherpesvirus MHV68

Jean Lee[*,‡‡], **Emily Cullum**[†,‡‡], **Kyle Stoltz**[‡,‡‡], **Niklas Bachmann**[§], **Zoe Strong**[¶], **Danielle D. Millick**[‖], **Lisa K. Denzin**[‖,#], **Anthony Chang**[¶], **Vera Tarakanova**[‡], **Alexander Chervonsky**[†,¶,**,††], **Tatyana Golovkina**[†,§,**,††]

[*]Committee on Cancer Biology, The University of Chicago, Chicago, IL, 60637

[†]Committee on Immunology, The University of Chicago, Chicago, IL, 60637

[‡]Microbiology and Immunology, Medical College of Wisconsin, Milwaukee, WI 53226

[§]Department of Microbiology, The University of Chicago, Chicago, IL, 60637

[¶]Department of Pathology, The University of Chicago, Chicago, IL, 60637

[‖]Graduate School of Biomedical Sciences, Rutgers University, Piscataway, NJ 08854

[#]Child Health Institute of NJ, Department of Pediatrics and Pharmacology, Rutgers Robert Wood Johnson Medical School, The State University of NJ, New Brunswick, NJ, 08901

[**]Committee on Microbiology, The University of Chicago, Chicago, IL, 60637

Abstract

H2-O (human HLA-DO) is a relatively conserved non-classical Major Histocompatibility Class II (MHCII)-like molecule. H2-O interaction with H2-M (human HLA-DM) edits the repertoire of peptides presented to T cell receptors by MHCII. It was long hypothesized that H2-M inhibition by H2-O provides protection from autoimmunity by preventing binding of the high affinity self-peptides to MHCII. The available evidence supporting this hypothesis, however, was inconclusive. A possibility still remained that the effect of H2-O-deficiency on autoimmunity could be better revealed by using H2-O-deficient mice that were already genetically predisposed to autoimmunity. Here, we generated and used autoimmunity-prone mouse models for systemic lupus erythematosus and organ-specific autoimmunity (Type 1 diabetes and multiple sclerosis) to definitively test whether H2-O prevents autoimmune pathology. Whereas our data failed to support any significance of H2-O in protection from autoimmunity, we found that it was critical for controlling a γherpesvirus, MHV68. Thus, we propose that H2-O editing of MHCII peptide repertoire may have evolved as a safeguard against specific highly prevalent viral pathogens.

[††]Address correspondence to T. Golovkina, Tel. (773) 8347988; tgolovki@bsd.uchicago.edu and A. Chervonsky, Tel (773)7021371: achervon@bsd.uchicago.edu.

Author contributions

J.L., E.C. and N.B. assisted in producing and genotyping NOD.$Ob^{-/-}$ and B6.NZM.$Ob^{-/-}$ mice. E.C. performed biochemical experiments and conducted EAE studies at the U of C. D.D.M conducted EAE studies at Rutgers. J.L. was assisted by N.B and Z.S. in performing flow cytometry experiments, ELISA and tissue staining. L.K.D performed flow cytometry experiments. A.C. performed scoring of renal pathology. K.S. and V.T. performed experiments with MHV68. E.C., T.G and A.V.C wrote the manuscript. J.L., N.B., Z.S., K.S., V. T. and L.K.D edited the manuscript. T.G. and A.V.C. conceived the project, guided the genetic crosses, contributed to all experiments.

[‡‡]These authors contributed equally

INTRODUCTION

The immune system has to maintain a delicate balance between efficient defense against pathogens and self-damaging inflammation. During an infection, pathogen-derived peptides are presented on the surface of professional antigen presenting cells (APCs) by major histocompatibility class II (MHCII) molecules to $CD4^+$T cells to initiate the adaptive immune response. Peptide loading of MHCII molecules occurs in the endosomes and lysosomes of APCs and is catalyzed by H2-M, a non-classical MHCII-like heterodimer (1). The final MHCII peptide array, however, is fine-tuned by another MHCII-like heterodimer, H2-O, which binds to H2-M and inhibits its function (2–4).

H2-O is an obligate αβ heterodimer, which in mice is encoded by the *H2-Oa* (*Oa*) and *H2-Ob* (*Ob*) genes (5). Biochemical, structural, and functional analyses all supported the role of H2-O as a negative regulator of immune responses (2, 3, 6–8). Moreover, H2-O-deficient mice and rare humans carrying loss-of-function alleles of DO generate potent neutralizing antibody responses against several viruses supporting this idea (9, 10).

Negative regulation of immunity by H2-O/DO led to prediction of its role as a guardian against autoimmunity, suggesting that autoimmune reactions should be found in H2-O/DO-deficient organisms. However, experimental evidence for autoimmunity in H2-O-deficient mice was not entirely compelling: the appearance of IgG2a anti-nuclear antibodies (4) was not confirmed by others (3, 9); whereas a report of an enhanced development of experimental autoimmune encephalomyelitis (EAE) in B6.$Oa^{-/-}$ mice (11) had an unusually low disease score in the wild-type control mice. However, the possibility still remained that a role for H2-O in preventing autoimmunity could be more definitively shown in mice from autoimmune-prone backgrounds.

Experimental mouse models of autoimmunity have been developed for numerous human diseases, including organ-specific and systemic models. Spontaneous models of autoimmunity are of particular interest as they recapitulate many features of human diseases and are controlled by multiple (known and unknown) genes. Two broadly used models, the non-obese diabetic (NOD) mouse model of Type 1 diabetes (T1D) and the C57BL/6J.NZM (B6.NZM) model of systemic lupus erythematosus (SLE) (12), display these characteristics. Other models of autoimmunity rely on induction of disease *via* immunization, cell transfer, or other experimental manipulations. One example is an induction of experimental autoimmune encephalomyelitis (EAE) in B6 mice immunized with MOG peptide in the presence of pertussis toxin (13).

To conclusively and definitively establish a role (or a lack thereof) for H2-O in autoimmunity, we used these three mouse models to test whether H2-O-deficiency would result in accelerated and/or exacerbated disease phenotypes. We found no significant enhancement of the disease phenotype in H2-O-deficient mice in all three models. Instead, we found that H2-O-deficient mice had an increased susceptibility to γ-herpesvirus MHV68. Therefore, we have to conclude that the function of H2-O is not in prevention of autoimmunity but is likely in controlling chronic viral infections.

Materials and Methods

Mice

NOD/ShiLtJ (NOD), C57BL/6J (B6), B6;NZM-*Sle1*$^{NZM2410/Aeg}$ *Sle2*$^{NZM2410/Aeg}$ *Sle3*$^{NZM2410/Aeg}$/LmoJ

(B6.NZM) mice were purchased from The Jackson Laboratory (TJL). B6.*Ob*$^{-/-}$ produced by us (9) were maintained at The University of Chicago, at Rutgers University and at Medical College of Wisconsin (MCW). B6.*Oa*$^{-/-}$ mice (3) were maintained at Rutgers University. NOD.*Ob*$^{-/-}$ mice were produced at Transgenic Facility of The University of Chicago using CRISPR/Cas9 technology. The 5'CTGTAGATGTCACCAAGCTC3' guide targeting exon 3 was used to produce NOD.*Ob*$^{-/-}$ mice. Mice from one line (#19), which have a 22bp deletion in the exon 3, were used in the studies. Founder of the line mouse #19 was crossed to NOD mice to ensure the germ-line transmission of the KO allele. Heterozygous female mice were crossed to homozygous males to generate homozygous and heterozygous mice inheriting the same microbiota from their mothers.

B6.NZM mice were crossed to B6.*Ob*$^{-/-}$ and resulting B6.NZM.*Ob*$^{-/+}$ mice were intercrossed to obtain B6.NZM.*Ob*$^{-/-}$ and B6.NZM.*Ob*$^{+/+}$ mice. PCRs specific for the NZM *Sle1/2/3* loci mapped to chromosomes 1, 4, and 7 were done with primers at proximal, intermediate and distal locations of each of the loci using the following primers. Proximal *Sle1* forward: GTGTCTGCCTTTGCACCTTT; proximal *Sle1* reverse: 5'CTGCTGTCTTTCCATCCACA3'. Intermediate *Sle1* forward: 5'TCCACAGAACTGTCCCTCAA3'; intermediate *Sle1* reverse: 5'ATACACTCACACCACCCCGT3'; Distal *Sle1* forward: 5'CTGACCTCCACACGACCC3'; distal *Sle1* reverse: 5'GCTTGGGAAACTGGATGAAA3'. Proximal *Sle2* forward: 5'TGGCCAACCTCTGTGCTTCC3'; proximal *Sle2* reverse: 5'ACAGTTGTCCTCTGACATCC3'. Intermediate *Sle2* forward: 5'GGCTTTGCAATGCTATGCAT3'; intermediate *Sle2* reverse: 5'TGGCAGGAGGTATGACAGAA3'. Distal *Sle2* forward: 5'GCTTGCTTTAGGAGTGTGCC3'; distal *Sle2* reverse: 5'TATTTGCTCTCCATTTCCCC3'. Proximal *Sle3* forward: 5'CCAGACCATCTGATCCAGATC3'; proximal *Sle3* reverse: 5'GGAGGTTGCAGTGAATTCAAG3'. Intermediate *Sle3* forward: 5'CCCACCAGAGATCACCAAGT3'; intermediate Sle3 reverse: 5'CACAATGAAGGCTGAAAGCA3'. Distal *Sle3* forward: 5'CACTTGGGGAACGTCAAGAC3'; distal *Sle3* reverse: 5'TGTAGACCATAGCCCATAAGCC3'. Only PCRs with distal and proximal primers are shown in Figure S1A.

Between 6–7 weeks of age mice were intranasally inoculated with 1000 plaque forming units (PFU) of MHV68 (WUMS) diluted in sterile serum-free Dulbecco's modified Eagle's medium (DMEM) (15μl/mouse), under light anesthesia. MHV68 viral stock was prepared and titered on NIH 3T12 cells. The spleens were harvested from euthanized mock-treated

and MHV68-infected animals at 16 days post infection. Mice were euthanized by CO_2 inhalation from a compressed gas source in a non-over-crowded chamber.

The studies described here have been reviewed and approved by the Animal Care and Use Committees at The University of Chicago, Rutgers University and MCW which are accredited by the Association for Assessment and Accreditation of Laboratory Animal Care (AAALAC).

Western blotting

Pellets of 1×10^7 red blood cell-depleted splenocytes were lysed in 20 mM Tris-HCl, 130 mM NaCl pH 7.4 containing 1% Triton X-100 and protease inhibitor cocktail (Roche Life Sciences) for 30 minutes on ice. Following centrifugation to eliminate nuclei and cellular debris, lysates were incubated at 98°C for 10 min in Laemmli buffer and resolved on a 15% SDS-PAGE gel (BioRad). After electrotransfer, PVDF membranes were blocked in 5% non-fat dry milk and incubated with a rabbit serum to the cytoplasmic tails of Mβ (R.Mb/c; see below) or Oβ [R.Ob/c (14)], or β-actin (clone AC-74; Sigma). The membranes were washed and probed with HRP-conjugated anti-rabbit Ig secondary Abs (Jackson ImmunoResearch). After extensive washing, blots were developed with chemiluminescent peroxidase substrate and visualized by Image LAS 3000 (FujiFilms).

Polyclonal Abs to the Mβ cytoplasmic tail (R.Mb/c) were produced in rabbits after multiple immunizations with a peptide encoding the Mβ cytoplasmic tail (Mβ/c; YTPLSGSTYPEGRH) conjugated to keyhole limpet hemocyanin. Mβ/c-specific Abs were purified from the sera by affinity chromatography with an Mβ/c peptide column.

EAE induction

The $MOG_{35–55}$/CFA Emulsion PTX kit for EAE induction was purchased from Hooke Laboratories and was used according to the manufacturer protocol. Male and female mice between the ages of 9 and 12 weeks were used in these studies. Mice were monitored for 28 days after EAE induction using the company's scoring guide. In experiments performed at Rutgers University, litters of B6.$Oa^{-/-}$ and wildtype B6J pups or B6.O$b^{-/-}$ and wildtype B6J pups were mixed and cross-fostered in two groups on B6 dams to normalize the microbiota. For experiments at U of C either $Ob^{+/+}$ littermates of $Ob^{-/-}$ mice (sharing the microbiota source) or B6J mice purchased from TJL were used as control.

FACS analysis

To measure T cell activation, red blood cells-depleted splenocytes were stained with: anti-CD4 (eBioscience), anti-CD8a (Invitrogen), anti-CD62L (BioLegend), anti-CD44 (BioLegend), anti-CD69 (Invitrogen) Abs in the presence of Fc-Block (BD Biosciences). To compare B cells subpopulations, the same samples were stained with: anti-B220 (BioLegend), anti-CD93 (BioLegend), anti-CD23 (BioLegend), anti-IgM (Invitrogen), anti-CD21/35 (BioLegend) and anti-CD1d (Invitrogen) Abs in the presence of Fc-Block. To compare Tfh, Tfr and Treg cell populations, the samples were stained with: anti-CD4 (BioLegend), anti-CXCR5 (BioLegend), anti-PD-1 (Invitrogen), anti-Foxp3 (Invitrogen) and anti-Bcl6 (Invitrogen). All stainings mentioned above were preceded by incubating

cells with Fc-Block (BD Biosciences). For intracellular staining, cells were permeabilized using Foxp3/Transcription factor staining buffer (Invitrogen). Dead cells were gated out by staining with Propidium Iodide (Sigma-Aldrich) or Zombie Aqua (BioLegend). For MHV68 studies, the following antibodies were used: anti-CD3, anti-CD4, anti-CD95, anti-PD-1, anti-B220, anti-GL7, anti-IgD, anti-IRF-4, anti-CD19, anti-CD11b and anti-CD11c (all from BioLegend) and anti-CXCR5 (BD Pharmingen). Intracellular staining for MHV68 studies was performed using BD Cytofix/Cytoperm kit (Fisher Scientific). Data were acquired using Fortessa or LSR-II flow cytometers (Becton, Dickinson & Company). Data analysis was performed using *FlowJo*™ software (Becton, Dickinson & Company).

Cryosectioning and Immunohistochemistry

Kidney samples embedded in O.C.T. (Sakura Tissue Tek®) were cut with cryostat into 8μm-thick sections, which were transferred to microscope slides. Slides were fixed in −20°C acetone, dried and stained with TRITC-coupled anti-mouse IgG (Jackson ImmunoResearch) or anti-mouse FITC-labeled C3a antibody (MP Biomedicals, LLC) in FACS buffer (1%FBS, 0.02% NaN_3 in PBS). After washes in FACS buffer, slides were wetted with 50% glycerol and covered with coverglass (IMEB Inc). The slides were stored at 4°C until imaging using DMLB microscope (Leica Microsystems IR GmbH) equipped with SPOT camera (Diagnostic Instruments, Inc.)

Anti-nuclear antibody (ANA) staining

HEp-2 slides (Bio-Rad) were incubated with serum samples diluted at 1:100 in FACS buffer and counterstained with TRITC-labeled donkey anti-mouse IgG (Jackson ImmunoResearch) diluted at 1:100 in FACS buffer. After washes in FACS buffer, slides were wetted with 50% glycerol and covered with coverglass (IMEB Inc). The imaging and scoring were performed on the Leica DMLB fluorescent microscope.

Mouse genomic DNA extraction, genotyping, and sequencing

Mouse genomic DNA was extracted from toe or ear samples using DirectPCR Lysis Reagent (Viagen Biotech) according to the manufacturer's protocol and subjected to PCR. The PCRs products were separated on 5% acryl-amide gel (Bio-Rad). For genomic analysis of the NOD.*Ob* KO allele, the PCR reactions were treated with ExoSAP-IT (Thermo Fisher Scientific) before submitting for sequencing.

Diabetes tracking

Diabetes development was monitored by weekly testing of urine glucose with Diastix strips (Bayer, Elkhart, IN).

Histology

Insulitis was scored on ≥100 islets/pancreas using 5μm, H&E-stained sections with 40μm intervals and scored as follows: 0, no visible infiltration; 1, peri-insulitis; 2, insulitis with <50% islet infiltration; 3, insulitis with >50% islet infiltration. Kidney pathology was scored using 5μm, PAS-stained sections with 40μm intervals and scored as follows by a renal pathologist: 0, no visible change; 1, focal mesangial proliferative changes; 2, diffuse

mesangial proliferative disease; 3, diffuse proliferative GN with focal crescents; 4, diffuse GN with crescents in >50% of glomeruli.

Viral Infections

Wild-type (WT) MHV68 (15) and MHV68.LANA:βlac (16) viruses were grown and tittered on 3T12 fibroblasts. Mice were infected intranasally with 10^3 PFUs of WT MHV68 or intraperitoneally (i.p.) with 10^6 PFUs of WT MHV68 or MHV68.LANA:βlac. Peritoneal cells were collected by lavage at 3 days post infection and subjected to flow analyses.

Limiting Dilution Assays

Frequency of virally infected nucleated cells (cells harboring viral DNA) was determined by limiting dilution PCR analysis; the frequency of *ex-vivo* reactivation to identify cells capable of producing infectious virus was determined by limiting dilution assay as previously described (17). Briefly, to determine the frequency of cells harboring viral DNA, splenocytes were pooled from all mice within each experimental group (3–5 mice/group) and 6 serial 3-fold dilutions were subjected to a nested PCR reaction (12 replicates/dilution) using primers against viral genome. To determine the frequency of cells reactivating virus *ex vivo*, serial two-fold dilutions of splenocytes harvested from infected mice were plated onto monolayers of mouse embryonic fibroblasts (MEF) immediately following harvest, at 24 replicates per dilution. MHV68 was allowed to reactivate from primary cells, and virus was further amplified within the same well *via* subsequent replication in MEF. At 21 days post-plating all replicates and dilutions were scored in a binary fashion for the presence of live fibroblasts (no viral reactivation/replication) or absence of such (as a result of cytopathic effect driven by lytic replication). Because primary MEF were used to amplify the virus, the sensitivity of limiting dilution reactivation assay was below a single PFU of MHV68 defined using cell-line plaque assay. Because the endpoint of viral amplification in MEF was measured, the limiting dilution reactivation assay was not susceptible to variability of titers released from primary cells upon viral reactivation *ex vivo*.

RESULTS

H2-O does not protect against spontaneous organ-specific autoimmunity

Developed in the 1970s, the NOD mouse model of T1D has been used extensively for understanding the genetic contributions to T1D (18). T1D development in mice from this strain is dependent on multiple insulin-dependent diabetes (*Idd*) genetic loci (19). The major contributor to T1D is *Idd1*, which contains the MHC genes on chromosome 17. The unique NOD MHC haplotype, $H2^{g7}$, is critical for development of diabetes in this strain (20). In order to test whether H2-O deficiency would accelerate diabetes development in NOD mice, we used a CRISPR/Cas9 approach to produce H2-O-deficient NOD mice (Figure 1A). Targeting of the *Ob* gene led to the loss of Oβ protein but did not affect the levels of H2-M (Figure 1B). Diabetes development in NOD mice is a sexually dimorphic trait more penetrant in females (21, 22) and thus, diabetes incidence was tracked in female mice. Female NOD.$Ob^{+/-}$ and NOD.$Ob^{-/-}$ littermates had no difference in onset of overt diabetes or in overall disease penetrance (Figure 2A). Infiltration of the pancreatic islets by immune cells is a prerequisite to diabetes development (22). To determine if insulitis was

exacerbated in H2-O-deficient mice, H&E-stained sections from 13-week-old NOD.$Ob^{-/-}$ and NOD.$Ob^{-/+}$ mice were scored (Figures 2B and 2C). The differences in the distribution of insulitis scores observed between H2-O-deficient and H2-O-sufficient mice were not significant. If anything, NOD.$Ob^{-/-}$ mice had mildly reduced islet infiltration compared to NOD.$Ob^{+/-}$ mice. Taken together, these data demonstrate that H2-O does not influence the progression of T1D in NOD mice.

H2-O does not protect against spontaneous systemic autoimmunity

To address the contribution of H2-O to a systemic autoimmune disease, the New Zealand Mixed (NZM) B6J (B6.NZM) tri-congenic model was used. B6.NZM mice resulted from the transfer of three systemic lupus erythematosus (*Sle*) loci identified in New Zealand White (NZW) and New Zealand Black (NZB) onto the B6J background (23). The hybrid NZM mouse is highly susceptible to an SLE-like disease which includes production of anti-nuclear Abs and glomerulonephritis (12, 23). Similar to NOD mice, SLE development in B6.NZM mice is a sexually dimorphic trait and is more penetrant in females (12). Mice from the B6.NZM strain are overall B6J genetically with three loci, *Sle1, Sle2*, and *Sle3* present on chromosomes 1, 4, and 7, respectively, derived from NZM mice (12, 24, 25). These mice possess the $H2^b$ haplotype of MHC like that of the conventional B6 mice (12). To generate H2-O deficient B6.NZM mice, we crossed B6.NZM to B6.$Ob^{-/-}$ and confirmed that these mice lacked Oβ, and thus H2-O, via Western blotting (Figure 1B) and had *Sle1-3* loci of the NZM background via PCR (Figure S1A).

Female $Ob^{+/+}$ and $Ob^{-/-}$ B6.NZM mice were studied for three major autoimmune phenotypes at 8 months of age: 1) antinuclear antibody (ANA) titers (Figure 3A), 2) kidney glomerulonephritis (Figures 3B and S1B), and 3) kidney IgG and C3 complement deposition (Figures 3C and 3D). Measurement of these hallmarks of SLE-like autoimmune disease in multiple organ systems showed no differences between H2-O-deficient and -sufficient mice. Furthermore, no differences in splenic immune cell activation, a known and measurable precursor for SLE disease in B6.NZM mice (26–28), were observed. The frequencies of splenic T regulatory cells (Tfr), T follicular helper cells (Tfh) and T follicular regulatory cells (Figures 3E, F and S1C) were similar between $Ob^{-/-}$ and $Ob^{+/+}$ B6.NZM mice. Furthermore, no significant differences were noted in frequencies of $CD69^+$ activated $CD4^+$ (Figure 3G) or in frequencies of activated and effector/effector memory $CD8^+$ T cells (Figures S1C). The absolute numbers of the $CD4^+$ T cell subsets from Figure 3E–G, were also similar between the wild-type and the knock-out animals (Figure S1D). Follicular B cells and marginal zone B cells were present at similar frequencies (Figure 3H, I) and numbers (Figure S1E) in the spleens of $Ob^{-/-}$ and $Ob^{+/+}$ B6.NZM mice. Of all parameters measured, only splenic $CD4^+$ effector/effector memory T cells were slightly but significantly elevated in $Ob^{-/-}$ compared to $Ob^{+/+}$ B6.NZM mice (Figure 3J and S1F). This difference was not observed between age-matched B6.$Ob^{-/-}$ and B6.$Ob^{+/+}$ mice (Figure 3J) and, thus, was attributable to the H2-O-deficiency on the NZM background. In the absence of any evidence for augmented autoimmune pathology, however, the physiological relevance of this elevation in $CD4^+$ activated memory T cells remains unclear. Overall, our data indicate that H2-O deficiency does not exacerbate SLE-like pathology in the B6.NZM model of autoimmunity.

H2-O does not protect against induced autoimmunity

In addition to models of spontaneous autoimmunity, we also tested whether H2-O deficiency would contribute to an acute onset of induced autoimmunity. EAE is a mouse model of multiple sclerosis (MS) and is induced by immunization of B6 mice (susceptible strain in this case) with a myelin oligodendrocyte glycoprotein (MOG) peptide emulsified in complete Freund's adjuvant (CFA) followed by the injection of pertussis toxin. MOG peptide is presented to T cells in the context of I-A^b MHCII molecules, thus allowing for the use of B6.$Ob^{-/-}$ and B6.$Oa^{-/-}$ mice in testing for the role of H2-O in development of the inflammation in the CNS. Autoimmune infiltration leads to an ascending paralysis beginning in the tail approximately 9 days post-immunization that progresses to the hind limb and, in some cases, forelimb paralysis several days after symptom onset. To test whether H2-O-deficient mice were differentially susceptible to EAE compared to H2-O-sufficient mice, EAE was induced by immunization in B6.$Oa^{-/-}$, B6.$Ob^{-/-}$ and control B6J mice. Immunized mice were monitored for the next 28 days for the symptoms of neuroinflammation. No statistically significant differences in disease development in H2-O-deficient (B6.$Ob^{-/-}$ mice) compared to H2-O-sufficient mice were observed when the data from all experimental mice from The University of Chicago and Rutgers University (both males and females) were combined (Figure 4A, B), or when only female mice were compared (Figure 4C, D). Similarly, B6.$Oa^{-/-}$ mice did not develop EAE disease with kinetics or severity that was different from their controls (Figure 4E, F). A recent study (11) found that B6.$Oa^{-/-}$ mice were more susceptible to EAE than control B6J animals. However, that conclusion was based on a single experiment, in which control B6J mice developed very mild EAE disease with an average score '1', which is far lower than the disease scores published by other groups (29–31) and also observed in our study. Thus, in this inducible model of autoimmunity, H2-O deficiency does not contribute to either disease development or severity.

H2-O contributes to control of a chronic γherpesvirus infection

Thus far we have not found a support for any substantial involvement of H2-O in prevention of autoimmunity. Moreover, our own findings in mice (9) and relevant human data (10) suggested that the loss of H2-O/HLA-DO function could be beneficial for promotion of strong neutralizing antiviral antibody responses. However, since H2-O is highly conserved throughout mammalian evolution (32, 33), its function must be important. To search for such a function, we broadened the scope of testing an importance of H2-O in viral infections.

For that, we turned to the mouse γherpesvirus 68 (MHV68, also known as murid herpesvirus 4), a natural rodent pathogen which shares high levels of genetic conservation with Epstein-Barr virus (EBV) and Kaposi Sarcoma-associated herpesvirus (KSHV) (15, 34, 35) infecting humans. Like EBV, MHV68 initially infects naïve B cells and drives both infected and bystander B cells to become germinal center (GC) B cells (36–38). Virally-induced GC B cells require Tfh cells (39, 40) and harbor both virus-specific and virus non-specific B cells. (39, 41, 42). These GC B cells transition to memory B cells that support life-long latent infection, or to plasma cells, where the viral 'latent to lytic' switch occurs (43, 44). After a brief acute lytic replication in a naive host, MHV68 establishes latency in several organs, including the spleen (45, 46). Viral latency in the spleen peaks

at 14 to 18 days post-infection, with most of the latent virus being present in the germinal center (GC) B cells (47, 48).

To determine if H2-O has a role in controlling γherpesvirus infection, B6.$Ob^{-/-}$ and B6.$Ob^{+/+}$ mice were infected with MHV68, and parameters of viral latency and reactivation were determined at 16 days post-infection. To compare the frequencies of latently infected splenic cells in B6.$Ob^{-/-}$ and B6.$Ob^{+/+}$ mice, we performed a limiting dilution PCR assay amplifying the MHV68 genome from pooled cells in multiple replicates. The frequency of latently infected cells in a given sample was determined by a number of cells added per well needed to achieve 62.5% MHV68 positivity of all replicates. Splenocytes from infected B6.$Ob^{-/-}$ mice contained about 6 times more latently infected cells as B6.$Ob^{+/+}$ splenocytes (Figure 5A). Similarly, for the *ex vivo* reactivation assay, splenocytes were added to microplate wells containing mouse embryonic fibroblasts (MEFs), and the cytopathic effect of the virus (loss of viable MEFs) was scored after three weeks of co-culture. The frequency of infected cells was determined similarly by the PCR assay. The viral reactivation was 5 times higher in B6.$Ob^{-/-}$ mice than in B6.$Ob^{+/+}$ mice (Figure 5B). Furthermore, flow cytometry analyses of individual spleens demonstrated that compared to B6.$Ob^{+/+}$ mice, B6.$Ob^{-/-}$ mice had significantly increased frequencies of GC B cells, Tfh cells, and class-switched plasma cells (Figures 5C–E, gating strategy is shown in Figure S3), reflecting the γherpesvirus-driven B cell differentiation. Thus, functional H2-O attenuates the establishment of chronic MHV68 infection. One possible caveat was a higher level of infection of susceptible cells in H2-O-deficient animals. That possibility was ruled out: frequencies of infected cells in the peritoneum of H2-O-positive and -negative mice infected with the virus via intraperitoneal injection were similar among the cells expressing H2-O (DC, B cells) and H2-O-negative macrophages (Figure S4).

DISCUSSION

By interacting with H2-M/HLA-DM, H2-O/HLA-DO edits the repertoire of peptides presented by MHCII to T cells. Indeed, small but significant differences were found in MHCII peptidomes between H2-O/DO-deficient and DO-sufficient cells with the latter containing many peptides that were absent from or present at much lower frequency in the H2-O/DO-deficient cells (11, 49). The data suggested a potential predisposition to autoimmunity in the absence of H2-O/DO due to an aberrant presentation of some high affinity self-peptides by MHCII or due to the loss of some low affinity tolerogenic peptides. Some findings of autoimmune phenotype (4) were not confirmed by others (3, 9), whereas other findings were obtained using control mice developing an underwhelming disease (11). Since we were not convinced that prevention of autoimmunity is the major function of H2-O/DO, we aimed at testing this hypothesis in three distinct disease models, in which H2-O deficiency was introduced in animals already prone to autoimmunity. That should have increased the chances to detect higher susceptibility of H2-O-deficient animals to autoimmunity. These models included spontaneous autoimmunity (T1D in NOD mice and SLE in B6.NZM mice), as well as induced autoimmunity (EAE in B6, B6.$Oa^{-/-}$ and B6.$Ob^{-/-}$ mice). In sum, except for a small increase in $CD4^+$ T cells with memory phenotype in B6.NZM.$Ob^{-/-}$ mice compared to B6.NZM mice (model of SLE), which had no visible effect on any other parameters of pathology reflecting disease severity, we

found no evidence in favor of H2-O being a negative regulator of autoimmunity. This small increase might be a result of interaction between *Ob* and an unknown gene mapped in one of the three SLE loci, which may be interesting to dissect in the future.

Interestingly, overexpression of human DO in NOD mouse dendritic cells led to the amelioration of T1D development (50). That was caused by propensity of human DO to suppress mouse H2-M function and, hence, presentation of diabetogenic peptides. Apparently, endogenous mouse H2-O that co-evolved with H2-M was not capable of reaching such level of suppression of H2-M function. This experiment underlies the importance of DO-DM interactions in editing self-peptides presented by MHCII. However, at the steady state, even if the loss of H2-O-mediated MHCII peptidome editing abrogates the removal of self-peptides that can drive autoimmune disease, other major mechanisms of self-tolerance (negative selection, lack of co-stimulatory signals, Tregs etc.) must be sufficient to prevent activation of autoreactive T and B cells.

Since our data do not support a role for H2-O as a protector from autoimmune disease development, we posit that the key to understanding the functions of H2-O/HLA-DO should be found by studying the involvement of these molecules in resistance to pathogens. However, this idea seemingly does not seat well with our own previous findings that H2-O-deficient mice produced potent neutralizing antibody responses against MMTV, a mouse retrovirus and some rare individuals with loss of function DOA and DOB alleles clear HCV and HBV (9, 10). Moreover, the presence of some gain of function alleles of DOA and DOB in humans correlated with persistence of HCV and HBV (9, 10). Therefore, the presence of functional H2-O/DO genes appears to benefit some pathogens and yet, these genes are highly conserved among all mammals (32). One reasonable explanation for H2-O/DO conservation throughout mammalian evolution could be in its possible role in protection from some highly prevalent pathogens. Such pathogens are likely to be intracellular, targeting MHCII-positive cells that can present an array of pathogen-derived peptides. Indeed, it has been found that mice of I/St strain carrying a defective *Ob* allele were uniquely sensitive to mycobacteria tuberculosis (MTB) compared to B6 and A/Sn mice carrying functional alleles of *Ob* (51–54). Although MTB can cause an antibody response (55), this response cannot provide pathogen clearance and could even become detrimental by enhancing pathogen uptake through Fc receptor-mediated phagocytosis (56). In the current study, we have identified one such microorganism – γherpesvirus MHV68, a prototype of cancer-associated human γherpesviruses such as EBV and Kaposi's Sarcoma-associated herpesvirus (KSHV) (57) which is controlled by H2-O.

γherpesviruses are highly prevalent in multiple mammalian species. These viruses infect B cells and rely on robust B cell differentiation reaction to establish a life-long infection of memory B cells (58). Although B cells are usurped by the virus as hosts of latent infection and viral reactivation, they are required as APCs (59) for inducing virus-specific $CD8^+$ (60–62). $CD4^+$ T cells have a dual role during γherpesvirus infection. Whereas $CD4^+$ T cells are proviral during establishment of latency [as they are required for GC reactions induced by the virus (40)], they also exert an anti-viral function controlling persistent virus by providing help to virus-specific $CD8^+$ T cells (63). We found that MHV68-mediated GC B cell and Tfh cell expansion was significantly increased in H2-O-deficient mice compared

to H2-O-sufficient mice (Figures 5C–5E) coinciding with a rise in the number of latently infected splenic cells (Figure 5A). Even though the virus is capable of infecting both B cells and myeloid cells, B cells are the most likely contributors to the overall rise in the latently infected cells as the ratio of B cells to myeloid cells in the spleen is about 40–70:1. These results indicate that proper expression of H2-O most likely in B cells puts the pressure on the virus during the establishment of latency restricting the overall pathogen burden.

Most of adults worldwide are chronically infected with EBV and KSHV reaches 50% seroprevalence in Sub-Saharan Africa and approximately 10% in central Europe or Northern America (57). These viruses can cause severe illnesses in immunocompromised patients however, they are well controlled by the immune system in most immunocompetent hosts. Our data suggest that the control of γherpesviruses is dependent on the presence and proper functioning of the HLA-DO. In addition, as H2-O expression is not restricted to B cells as it is also highly expressed in dendritic cells (14) and thymic epithelial cells (64), it is possible that H2-O may also contribute to control of chronic viruses infecting these cells.

The precise mechanism by which H2-O/DO control the establishment of viral latency is yet to be determined, but one can speculate that it is based on reduction of DM-dependent presentation of high affinity peptides leading to downregulation of GC reactions triggered by the $CD4^+$ T cells.

Supplementary Material

Refer to Web version on PubMed Central for supplementary material.

Acknowledgments

We are thankful to members of the Golovkina and Chervonsky laboratories for discussions and to Louis Osorio for technical assistance.

Funding sources:

This work was supported by PHS grant AI117535 to T. G. and L.K.D., by AI127411 to A.V.C., by P30 CA014599 to the University of Chicago, by the National Center for Advancing Translational Sciences of the National Institutes of Health through Grant Number UL1 TR000430 to the University of Chicago. Other support was provided by The Robert Wood Johnson Foundation (Grant 67038 to the Child Health Institute of New Jersey), and The Barile Children's Medical Research Trust (to L.K.D.).

References

1. Blum JS, Wearsch PA, and Cresswell P. 2013. Pathways of antigen processing. Annu Rev Immunol 31: 443–473. [PubMed: 23298205]
2. Denzin LK, Sant'Angelo DB, Hammond C, Surman MJ, and Cresswell P. 1997. Negative regulation by HLA-DO of MHC class II-restricted antigen processing. Science 278: 106–109. [PubMed: 9311912]
3. Liljedahl M, Winqvist O, Surh CD, Wong P, Ngo K, Teyton L, Peterson PA, Brunmark A, Rudensky AY, Fung-Leung WP, and Karlsson L. 1998. Altered antigen presentation in mice lacking H2-O. Immunity 8: 233–243. [PubMed: 9492004]
4. Gu Y, Jensen PE, and Chen X. 2013. Immunodeficiency and autoimmunity in H2-O-deficient mice. J Immunol 190: 126–137. [PubMed: 23209323]

5. Liljedahl M, Kuwana T, Fung-Leung WP, Jackson MR, Peterson PA, and Karlsson L. 1996. HLA-DO is a lysosomal resident which requires association with HLA-DM for efficient intracellular transport. The EMBO journal 15: 4817–4824. [PubMed: 8890155]
6. van Ham SM, Tjin EP, Lillemeier BF, Gruneberg U, van Meijgaarden KE, Pastoors L, Verwoerd D, Tulp A, Canas B, Rahman D, Ottenhoff TH, Pappin DJ, Trowsdale J, and Neefjes J. 1997. HLA-DO is a negative modulator of HLA-DM-mediated MHC class II peptide loading. Curr Biol 7: 950–957. [PubMed: 9382849]
7. Chen X, Laur O, Kambayashi T, Li S, Bray RA, Weber DA, Karlsson L, and Jensen PE. 2002. Regulated expression of human histocompatibility leukocyte antigen (HLA)-DO during antigen-dependent and antigen-independent phases of B cell development. J Exp Med 195: 1053–1062. [PubMed: 11956296]
8. Guce AI, Mortimer SE, Yoon T, Painter CA, Jiang W, Mellins ED, and Stern LJ. 2013. HLA-DO acts as a substrate mimic to inhibit HLA-DM by a competitive mechanism. Nature structural & molecular biology 20: 90–98.
9. Denzin LK, Khan AA, Virdis F, Wilks J, Kane M, Beilinson HA, Dikiy S, Case LK, Roopenian D, Witkowski M, Chervonsky AV, and Golovkina TV. 2017. Neutralizing Antibody Responses to Viral Infections Are Linked to the Non-classical MHC Class II Gene H2-Ob. Immunity 47: 310–322.e317. [PubMed: 28813660]
10. Graves AM, Virdis F, Morrison E, Alvaro-Benito M, Khan AA, Freund C, Golovkina TV, and Denzin LK. 2020. Human Hepatitis B Viral Infection Outcomes Are Linked to Naturally Occurring Variants of HLA-DOA That Have Altered Function. J Immunol 205: 923–935. [PubMed: 32690655]
11. Welsh RA, Song N, Foss CA, Boronina T, Cole RN, and Sadegh-Nasseri S. 2020. Lack of the MHC class II chaperone H2-O causes susceptibility to autoimmune diseases. PLoS Biol 18: e3000590. [PubMed: 32069316]
12. Morel L, Croker BP, Blenman KR, Mohan C, Huang G, Gilkeson G, and Wakeland EK. 2000. Genetic reconstitution of systemic lupus erythematosus immunopathology with polycongenic murine strains. Proceedings of the National Academy of Sciences 97: 6670–6675.
13. Lyons JA, San M, Happ MP, and Cross AH. 1999. B cells are critical to induction of experimental allergic encephalomyelitis by protein but not by a short encephalitogenic peptide. European Journal of Immunology 29: 3432–3439. [PubMed: 10556797]
14. Fallas JL, Yi W, Draghi NA, O'Rourke HM, and Denzin LK. 2007. Expression patterns of H2-O in mouse B cells and dendritic cells correlate with cell function. J Immunol 178: 1488–1497. [PubMed: 17237397]
15. Virgin HW, Latreille P, Wamsley P, Hallsworth K, Weck KE, Dal Canto AJ, and Speck SH. 1997. Complete sequence and genomic analysis of murine gammaherpesvirus 68. J. Virol 71: 5894–5904. [PubMed: 9223479]
16. Nealy MS, Coleman CB, Li H, and Tibbetts SA. 2010. Use of a virus-encoded enzymatic marker reveals that a stable fraction of memory B cells expresses latency-associated nuclear antigen throughout chronic gammaherpesvirus infection. Journal of virology 84: 7523–7534. [PubMed: 20484501]
17. Tarakanova VL, Stanitsa E, Leonardo SM, Bigley TM, and Gauld SB. 2010. Conserved gammaherpesvirus kinase and histone variant H2AX facilitate gammaherpesvirus latency in vivo. Virology 405: 50–61. [PubMed: 20557919]
18. Leiter E, and Atkinson M. 1998. Nod Mice and Related Strains: Research Applications in Diabetes, AIDS, Cancer, And Other Diseases R.G. Landes Company.
19. Driver JP, Serreze DV, and Chen Y-G. 2011. Mouse models for the study of autoimmune type 1 diabetes: a NOD to similarities and differences to human disease. Seminars in Immunopathology 33: 67–87. [PubMed: 20424843]
20. Miyazaki T, Uno M, Uehira M, Kikutani H, Kishimoto T, Kimoto M, Nishimoto H, Miyazaki J, and Yamamura K. 1990. Direct evidence for the contribution of the unique I-ANOD to the development of insulitis in non-obese diabetic mice. Nature 345: 722–724. [PubMed: 2113614]

21. Yurkovetskiy L, Burrows M, Khan AA, Graham L, Volchkov P, Becker L, Antonopoulos D, Umesaki Y, and Chervonsky AV. 2013. Gender bias in autoimmunity is influenced by microbiota. Immunity 39: 400–412. [PubMed: 23973225]
22. Makino S, Kunimoto K, Muraoka Y, Mizushima Y, Katagiri K, and Tochino Y. 1980. Breeding of a Non-Obese, Diabetic Strain of Mice. Experimental Animals 29: 1–13. [PubMed: 6995140]
23. Rudofsky UH, Evans BD, Balaban SL, Mottironi VD, and Gabrielsen AE. 1993. Differences in expression of lupus nephritis in New Zealand mixed H-2z homozygous inbred strains of mice derived from New Zealand black and New Zealand white mice. Origins and initial characterization. Lab Invest 68: 419–426. [PubMed: 8479150]
24. Morel L, Mohan C, Yu Y, Croker BP, Tian N, Deng A, and Wakeland EK. 1997. Functional dissection of systemic lupus erythematosus using congenic mouse strains. J Immunol 158: 6019–6028. [PubMed: 9190957]
25. Morel L, Yu Y, Blenman KR, Caldwell RA, and Wakeland EK. 1996. Production of congenic mouse strains carrying genomic intervals containing SLE-susceptibility genes derived from the SLE-prone NZM2410 strain. Mamm Genome 7: 335–339. [PubMed: 8661718]
26. Mohan C, Alas E, Morel L, Yang P, and Wakeland EK. 1998. Genetic dissection of SLE pathogenesis. Sle1 on murine chromosome 1 leads to a selective loss of tolerance to H2A/H2B/DNA subnucleosomes. J Clin Invest 101: 1362–1372.
27. Mohan C, Morel L, Yang P, and Wakeland EK. 1997. Genetic dissection of systemic lupus erythematosus pathogenesis: Sle2 on murine chromosome 4 leads to B cell hyperactivity. J Immunol 159: 454–465. [PubMed: 9200486]
28. Mohan C, Yu Y, Morel L, Yang P, and Wakeland EK. 1999. Genetic Dissection of Sle Pathogenesis: Sle3 on Murine Chromosome 7 Impacts T Cell Activation, Differentiation, and Cell Death. The Journal of Immunology 162: 6492–6502. [PubMed: 10352264]
29. Terry RL, Ifergan I, and Miller SD. 2016. Experimental Autoimmune Encephalomyelitis in Mice. Methods Mol Biol 1304: 145–160. [PubMed: 25005074]
30. Marusic S, Leach MW, Pelker JW, Azoitei ML, Uozumi N, Cui J, Shen MW, DeClercq CM, Miyashiro JS, Carito BA, Thakker P, Simmons DL, Leonard JP, Shimizu T, and Clark JD. 2005. Cytosolic phospholipase A2 alpha-deficient mice are resistant to experimental autoimmune encephalomyelitis. J Exp Med 202: 841–851. [PubMed: 16172261]
31. Mendel I, Kerlero de Rosbo N, and Ben-Nun A. 1995. A myelin oligodendrocyte glycoprotein peptide induces typical chronic experimental autoimmune encephalomyelitis in H-2b mice: fine specificity and T cell receptor V beta expression of encephalitogenic T cells. Eur J Immunol 25: 1951–1959. [PubMed: 7621871]
32. Flajnik MF 2018. A cold-blooded view of adaptive immunity. Nature reviews. Immunology 18: 438–453.
33. Kumanovics A, Takada T, and Lindahl KF. 2003. Genomic organization of the mammalian MHC. Annu Rev Immunol 21: 629–657. [PubMed: 12500978]
34. Efstathiou S, Ho YM, and Minson AC. 1990. Cloning and molecular characterization of the murine herpesvirus 68 genome. J. Gen. Virol 71: 1355–1364. [PubMed: 2351958]
35. Efstathiou S, Ho YM, Hall S, Styles CJ, Scott SD, and Gompels UA. 1990. Murine herpesvirus 68 is genetically related to the gammaherpesviruses Epstein-Barr virus and herpesvirus saimiri. J. Gen. Virol 71: 1365–1372. [PubMed: 2161903]
36. Coleman CB, Nealy MS, and Tibbetts SA. 2010. Immature and transitional B cells are latency reservoirs for a gammaherpesvirus. Journal of virology 84: 13045–13052. [PubMed: 20926565]
37. Flano E, Husain SM, Sample JT, Woodland DL, and Blackman MA. 2000. Latent murine gamma-herpesvirus infection is established in activated B cells, dendritic cells, and macrophages. J Immunol 165: 1074–1081. [PubMed: 10878386]
38. Thorley-Lawson DA 2001. Epstein-Barr virus: exploiting the immune system. Nature reviews. Immunology 1: 75–82.
39. Gauld SB, De Santis JL, Kulinski JM, McGraw JA, Leonardo SM, Ruder EA, Maier W, and Tarakanova VL. 2013. Modulation of B-cell tolerance by murine gammaherpesvirus 68 infection: requirement for Orf73 viral gene expression and follicular helper T cells. Immunology 139: 197–204. [PubMed: 23311955]

40. Collins CM, and Speck SH. 2014. Expansion of murine gammaherpesvirus latently infected B cells requires T follicular help. PLoS Pathog 10: e1004106. [PubMed: 24789087]
41. Sangster MY, Topham DJ, D'Costa S, Cardin RD, Marion TN, Myers LK, and Doherty PC. 2000. Analysis of the virus-specific and nonspecific B cell response to a persistent B-lymphotropic gammaherpesvirus. J Immunol 164: 1820–1828. [PubMed: 10657630]
42. Darrah EJ, Jondle CN, Johnson KE, Xin G, Lange PT, Cui W, Olteanu H, and Tarakanova VL. 2019. Conserved Gammaherpesvirus Protein Kinase Selectively Promotes Irrelevant B Cell Responses. Journal of virology 93.
43. Flano E, Kim IJ, Woodland DL, and Blackman MA. 2002. Gamma-herpesvirus latency is preferentially maintained in splenic germinal center and memory B cells. J Exp Med 196: 1363–1372. [PubMed: 12438427]
44. Matar CG, Rangaswamy US, Wakeman BS, Iwakoshi N, and Speck SH. 2014. Murine gammaherpesvirus 68 reactivation from B cells requires IRF4 but not XBP-1. Journal of virology 88: 11600–11610. [PubMed: 25078688]
45. Weck KE, Barkon ML, Yoo LI, Speck SH, and Virgin HI. 1996. Mature B cells are required for acute splenic infection, but not for establishment of latency, by murine gammaherpesvirus 68. Journal of virology 70: 6775–6780. [PubMed: 8794315]
46. Weck KE, Kim SS, Virgin HI, and Speck SH. 1999. Macrophages are the major reservoir of latent murine gammaherpesvirus 68 in peritoneal cells. Journal of virology 73: 3273–3283. [PubMed: 10074181]
47. Willer DO, and Speck SH. 2003. Long-term latent murine Gammaherpesvirus 68 infection is preferentially found within the surface immunoglobulin D-negative subset of splenic B cells in vivo. Journal of virology 77: 8310–8321. [PubMed: 12857900]
48. Collins CM, and Speck SH. 2012. Tracking murine gammaherpesvirus 68 infection of germinal center B cells in vivo. PLoS One 7: e33230. [PubMed: 22427999]
49. Nanaware PP, Jurewicz MM, Leszyk JD, Shaffer SA, and Stern LJ. 2019. HLA-DO Modulates the Diversity of the MHC-II Self-peptidome. Mol Cell Proteomics 18: 490–503. [PubMed: 30573663]
50. Yi W, Seth NP, Martillotti T, Wucherpfennig KW, Sant'Angelo DB, and Denzin LK. 2010. Targeted regulation of self-peptide presentation prevents type I diabetes in mice without disrupting general immunocompetence. J Clin Invest 120: 1324–1336. [PubMed: 20200448]
51. Nikonenko BV, Averbakh MM Jr., Lavebratt C, Schurr E, and Apt AS. 2000. Comparative analysis of mycobacterial infections in susceptible I/St and resistant A/Sn inbred mice. Tubercle and lung disease : the official journal of the International Union against Tuberculosis and Lung Disease 80: 15–25.
52. Korotetskaia MV, Kapina MA, Averbakh MM, Evstifeev VV, Apt AS, and Logunova NN. 2011. [A locus involved in tuberculosis infection control in mice locates in the proximal part of the H2 complex]. Mol Biol (Mosk) 45: 68–76. [PubMed: 21485498]
53. Keane TM, Goodstadt L, Danecek P, White MA, Wong K, Yalcin B, Heger A, Agam A, Slater G, Goodson M, Furlotte NA, Eskin E, Nellaker C, Whitley H, Cleak J, Janowitz D, Hernandez-Pliego P, Edwards A, Belgard TG, Oliver PL, McIntyre RE, Bhomra A, Nicod J, Gan X, Yuan W, van der Weyden L, Steward CA, Bala S, Stalker J, Mott R, Durbin R, Jackson IJ, Czechanski A, Guerra-Assuncao JA, Donahue LR, Reinholdt LG, Payseur BA, Ponting CP, Birney E, Flint J, and Adams DJ. 2011. Mouse genomic variation and its effect on phenotypes and gene regulation. Nature 477: 289–294. [PubMed: 21921910]
54. Denzin LK, Khan AA, Virdis F, Wilks J, Kane M, Beilinson HA, Dikiy S, Case LK, Roopenian D, Witkowski M, Chervonsky AV, and Golovkina TV. 2017. Neutralizing Antibody Responses to Viral Infections Are Linked to the Non-classical MHC Class II Gene H2-Ob. Immunity 47: 310–322 e317. [PubMed: 28813660]
55. Radaeva TV, Nikonenko BV, Mischenko VV, Averbakh MM Jr., and Apt AS. 2005. Direct comparison of low-dose and Cornell-like models of chronic and reactivation tuberculosis in genetically susceptible I/St and resistant B6 mice. Tuberculosis (Edinb) 85: 65–72. [PubMed: 15687029]
56. Ernst JD 1998. Macrophage receptors for Mycobacterium tuberculosis. Infection and immunity 66: 1277–1281. [PubMed: 9529042]

57. Cesarman E 2014. Gammaherpesviruses and lymphoproliferative disorders. Annu. Rev. Pathol 9: 349–372. [PubMed: 24111911]

58. Johnson KE, and Tarakanova VL. 2020. Gammaherpesviruses and B Cells: A Relationship That Lasts a Lifetime. Viral Immunol 33: 316–326. [PubMed: 31913773]

59. McClellan KB, Gangappa S, Speck SH, and Virgin H. W. t.. 2006. Antibody-independent control of gamma-herpesvirus latency via B cell induction of anti-viral T cell responses. PLoS Pathog 2: e58. [PubMed: 16789842]

60. Hu Z, Blackman MA, Kaye KM, and Usherwood EJ. 2015. Functional heterogeneity in the CD4+ T cell response to murine gamma-herpesvirus 68. J Immunol 194: 2746–2756. [PubMed: 25662997]

61. Sparks-Thissen RL, Braaten DC, Hildner K, Murphy TL, Murphy KM, and Virgin H. W. t.. 2005. CD4 T cell control of acute and latent murine gammaherpesvirus infection requires IFNgamma. Virology 338: 201–208. [PubMed: 15961135]

62. Tibbetts SA, van Dyk LF, Speck SH, and Virgin H. W. t.. 2002. Immune control of the number and reactivation phenotype of cells latently infected with a gammaherpesvirus. Journal of virology 76: 7125–7132. [PubMed: 12072512]

63. Cardin RD, Brooks JW, Sarawar SR, and Doherty PC. 1996. Progressive loss of CD8+ T cell-mediated control of a gamma-herpesvirus in the absence of CD4+ T cells. J Exp Med 184: 863–871. [PubMed: 9064346]

64. Karlsson L, Surh CD, Sprent J, and Peterson PA. 1991. A novel class II MHC molecule with unusual tissue distribution. Nature 351: 485–488. [PubMed: 1675431]

65. Riggs JB, Medina EM, Perrenoud LJ, Bonilla DL, Clambey ET, van Dyk LF, and Berg LJ. 2021. Optimized Detection of Acute MHV68 Infection With a Reporter System Identifies Large Peritoneal Macrophages as a Dominant Target of Primary Infection. Front Microbiol 12: 656979. [PubMed: 33767688]

Key Points

1. H2-O deficiency does not predispose to organ-specific or systemic autoimmunity
2. H2-O controls the establishment of a chronic γherpesvirus infection.

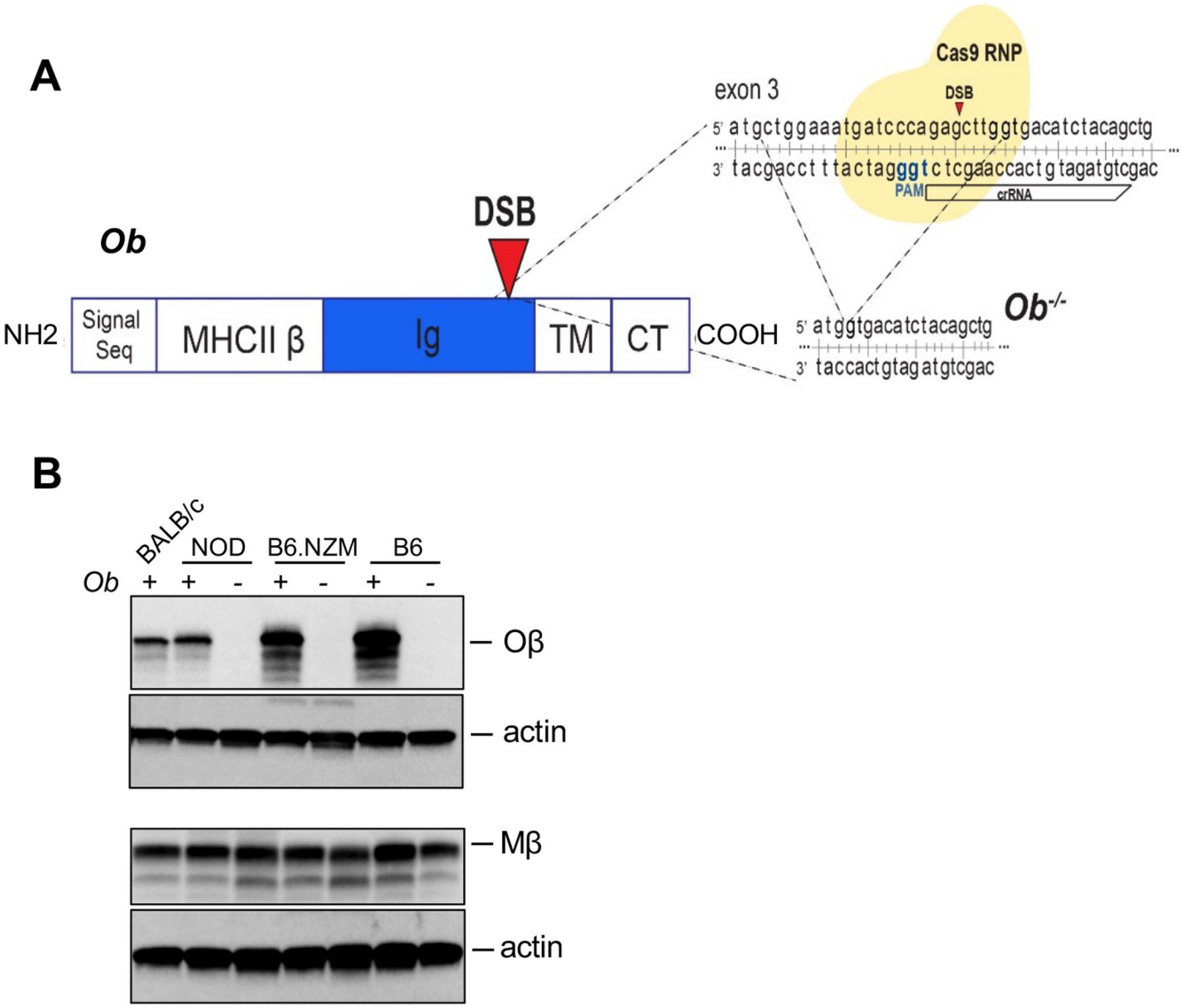

Figure 1. Generation of new H2-O-negative mouse models of autoimmunity.

A. CRISPR/Cas9 targeting strategy for generation of NOD.*Ob*$^{-/-}$ mice. Signal Seq, Signal sequence; MHCIIβ, MHCIIβ-like domain; Ig, Immunoglobulin domain; TM, Transmembrane region; CT, Cytoplasmic tail; DSB, Double strand break; gRNA, guide RNA. **B**. Loss of Oβ in novel H2-O knock-out lines. Splenocyte lysates from indicated mouse strains were analyzed by Western blotting with antibodies specific for the cytoplasmic tails of Mβ and Oβ proteins as well as with anti-β-actin antibodies (loading control). BALB/c splenocytes served as the control for NOD splenocytes as these strains carry an allele of *Ob* with the same CT sequence, which determines reactivity with anti-CT antibody. One of the 2 representative experiments.

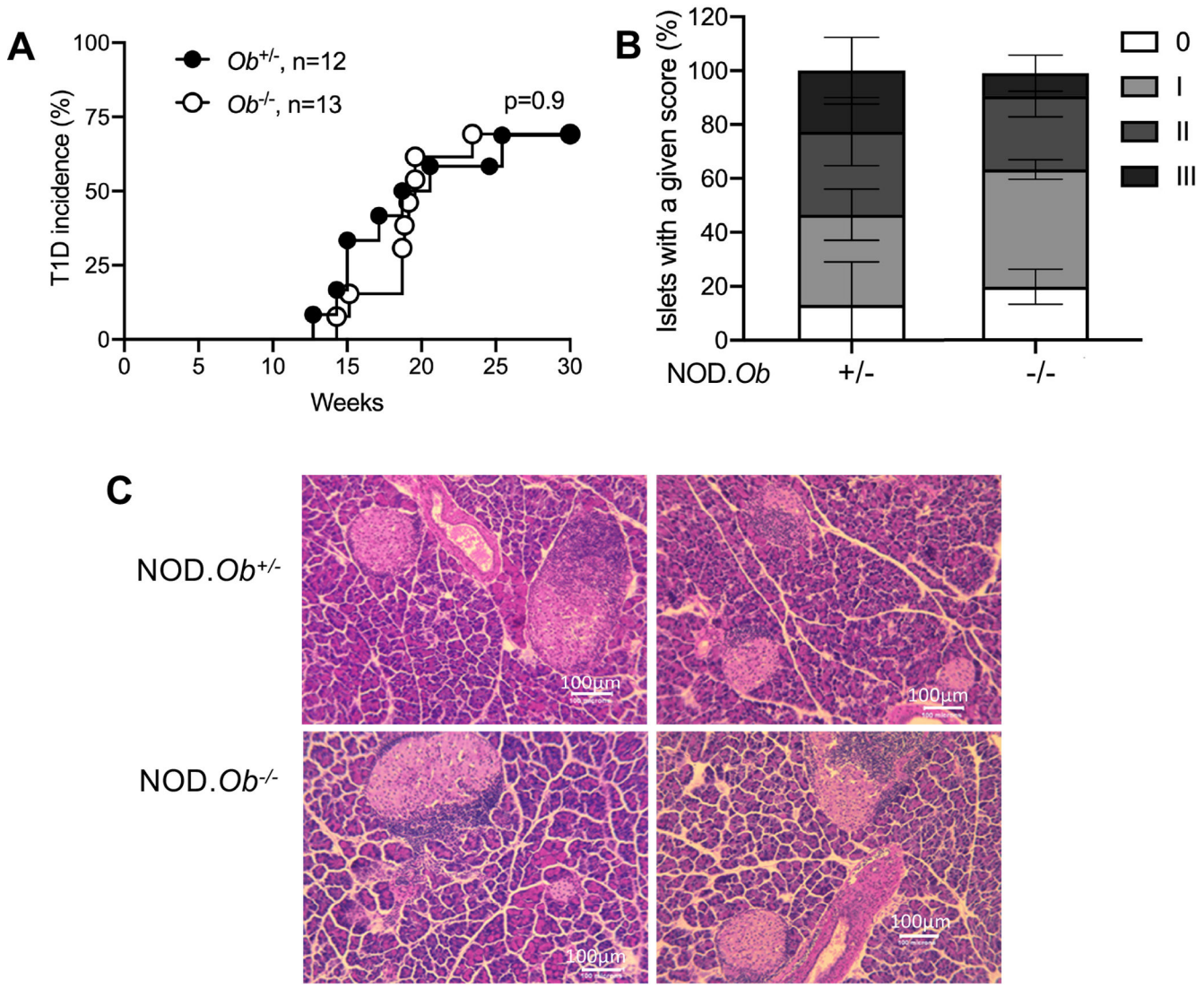

Figure 2. T1D development in H2-O-sufficient and H2-O-deficient NOD mice.

A. Cumulative T1D incidence of SPF NOD.*Ob*$^{+/-}$ and NOD.*Ob*$^{-/-}$ littermate females. Significance was calculated using log-rank Mantel-Cox test. ns, not significant (p>0.05). Data are a single observation experiment. n, number of mice used per group. **B**. Histopathology scores of islets from 13-wk-old nondiabetic females (n=5/group). Score 1, no visible infiltration; Score 2, peri-insulitis; Score 3, insulitis with <50% islet infiltration; Score 4, insulitis with >50% islet infiltration. **C**. Representative images of pancreatic islets from specific pathogen free 13-wk-old nondiabetic females.

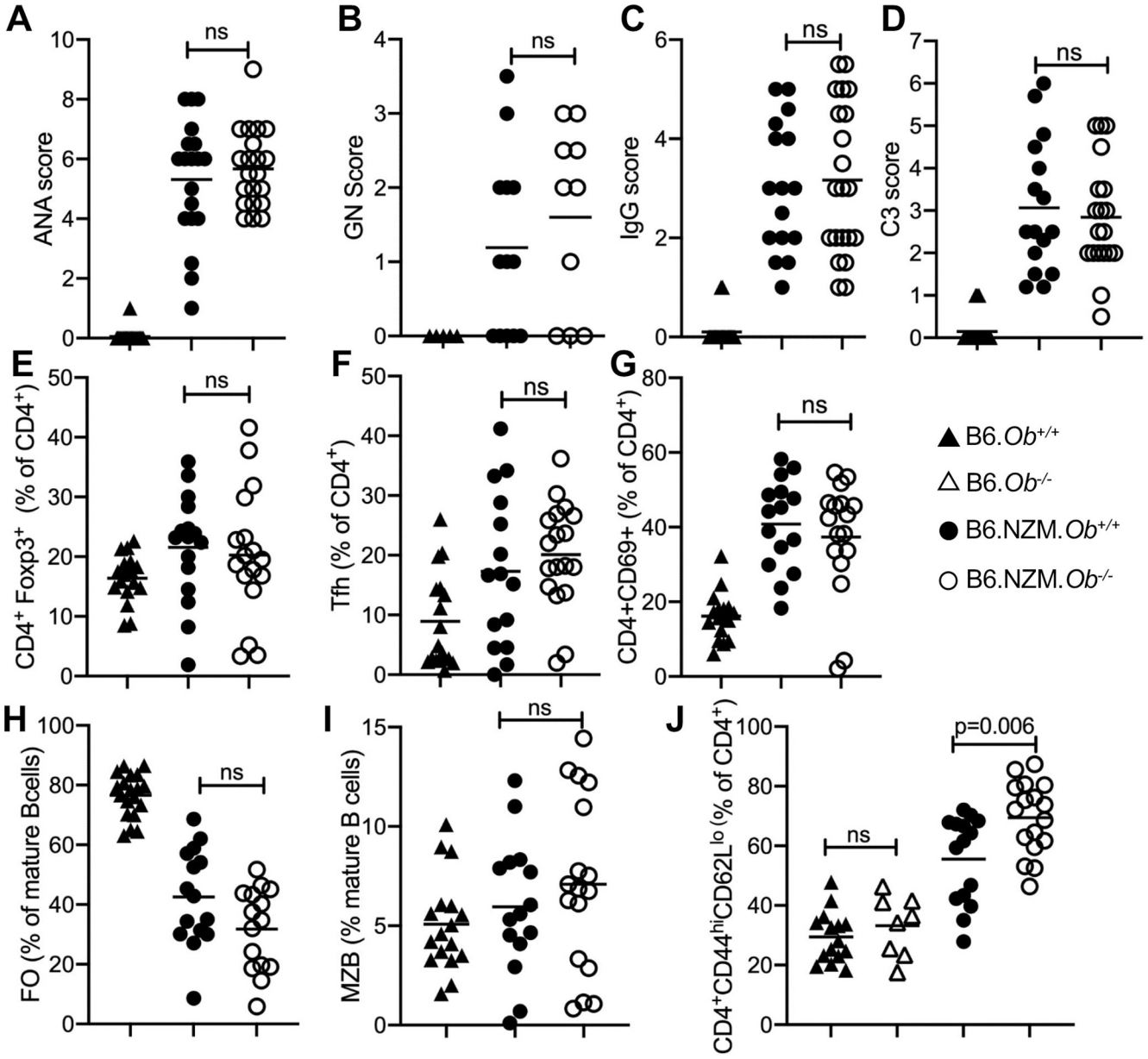

Figure 3. Comparison of SLE severity in B6.NZM and B6.NZM.*Ob*$^{-/-}$ mice.

A. Anti-nuclear antibody (ANA) scores measured by immunofluorescence of HEp-2 slides with sera diluted 1:100. **B**. Glomerulonephritis (GN) scores (see Figure S1B for representative histology pictures), **C** - IgG immune complex deposits and **D** - complement C3 deposits measured in kidneys using immunofluorescence. **E-J**, FACS analyses performed on splenocytes measuring populations indicated on the ordinates of the graphs. Gating strategies are shown in Figure S2. T follicular helper cells (Tfh) were defined as $CD4^+PD\text{-}1^+CXCR5^+BCL6^+FOXP3^-$; follicular B cells (FO) were defined as $CD93^-B220^+IgM^{lo}CD23^+$; and marginal zone B cells (MZB) were defined as $CD93^-B220^+IgM^{hi}CD23^-CD21^+CD1d^+$. All B cell subsets are shown as % of the total $CD93^-B220^+$ B cell population, $CD4^+$ T cell subsets as % of the total $CD4^+$ T cell population and $CD8^+$ T cell subsets as % of the total $CD8^+$ T cell population. All parameters

were measured with samples collected from 6–8-month-old females. Significance was calculated using an unpaired *t* test. ns, not significant (p>0.05). Twenty B6.$Ob^{+/+}$, 8 B6.$Ob^{-/-}$, 19 B6NZM.$Ob^{+/+}$ and 21 B6.NZM.$Ob^{-/-}$ mice were used in 6 independent experiments.

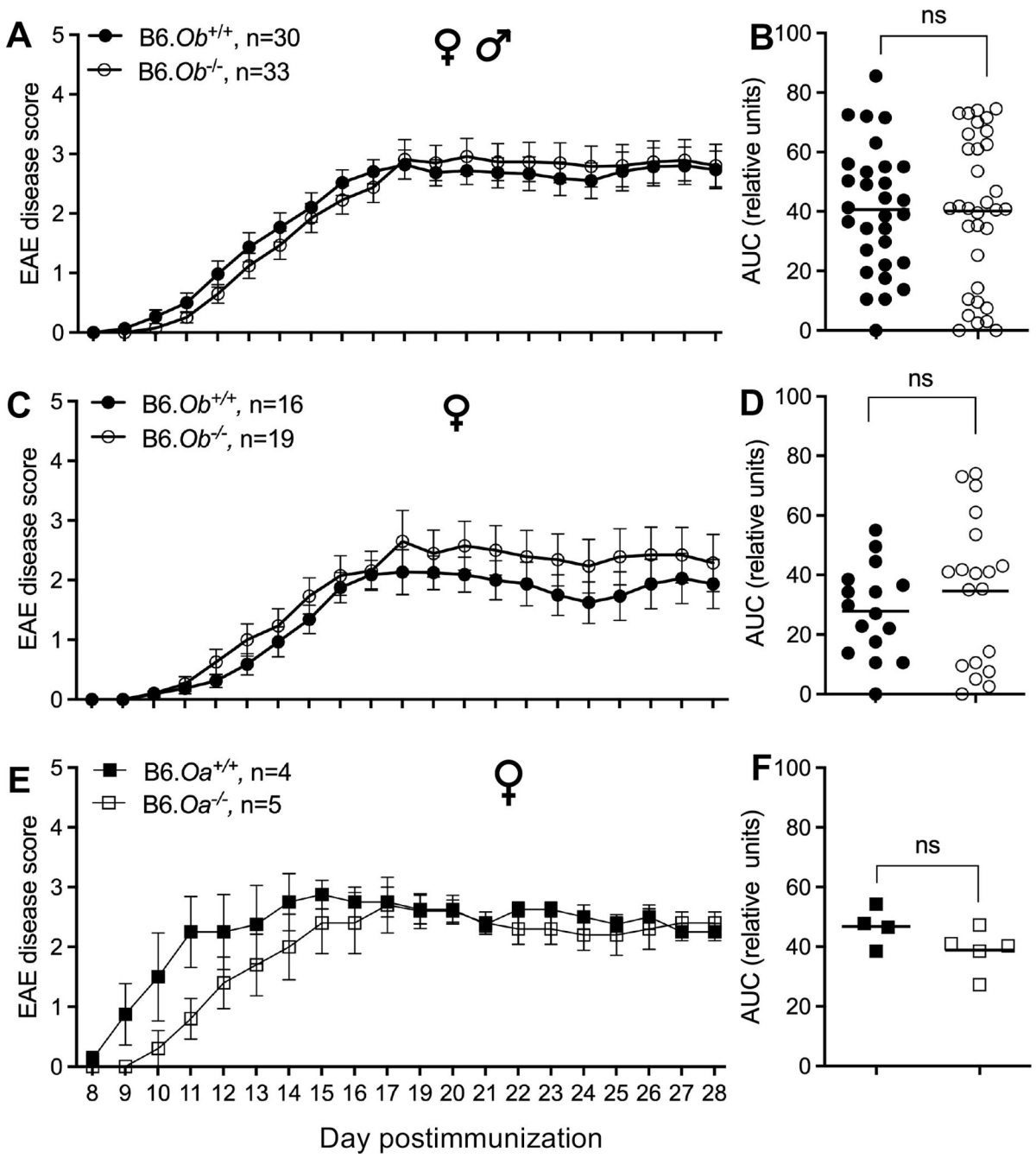

Figure 4. EAE development in B6 and B6.*Ob*$^{-/-}$ mice.

Disease scores (**A**) and area under the curve (AUC) analysis (**B**) for male and female B6.*Ob*$^{+/+}$ and B6.*Ob*$^{-/-}$ mice. Data combined from three independent experiments performed at two institutions. **C, D** show females only. **E, F** – similar analysis of B6.*Oa*$^{+/+}$ and B6.*Oa*$^{-/-}$ mice.

Mice were immunized with MOG35–55 in complete Freund's adjuvant (CFA) alongside pertussis toxin administration. Daily disease scoring started eight days after immunization. Score 0= no paralysis, 1= limp tail, 2= partial hind limb paralysis, 3= total hind limb paralysis, 4= partial forelimb and total hind limb paralysis, and 5= death. Significance was

calculated using an unpaired *t* test. Error bars indicate standard error of the mean. *=p≤ 0.05; **=p ≤0.01. ns, not significant (p>0.05). n, number of mice used per group.

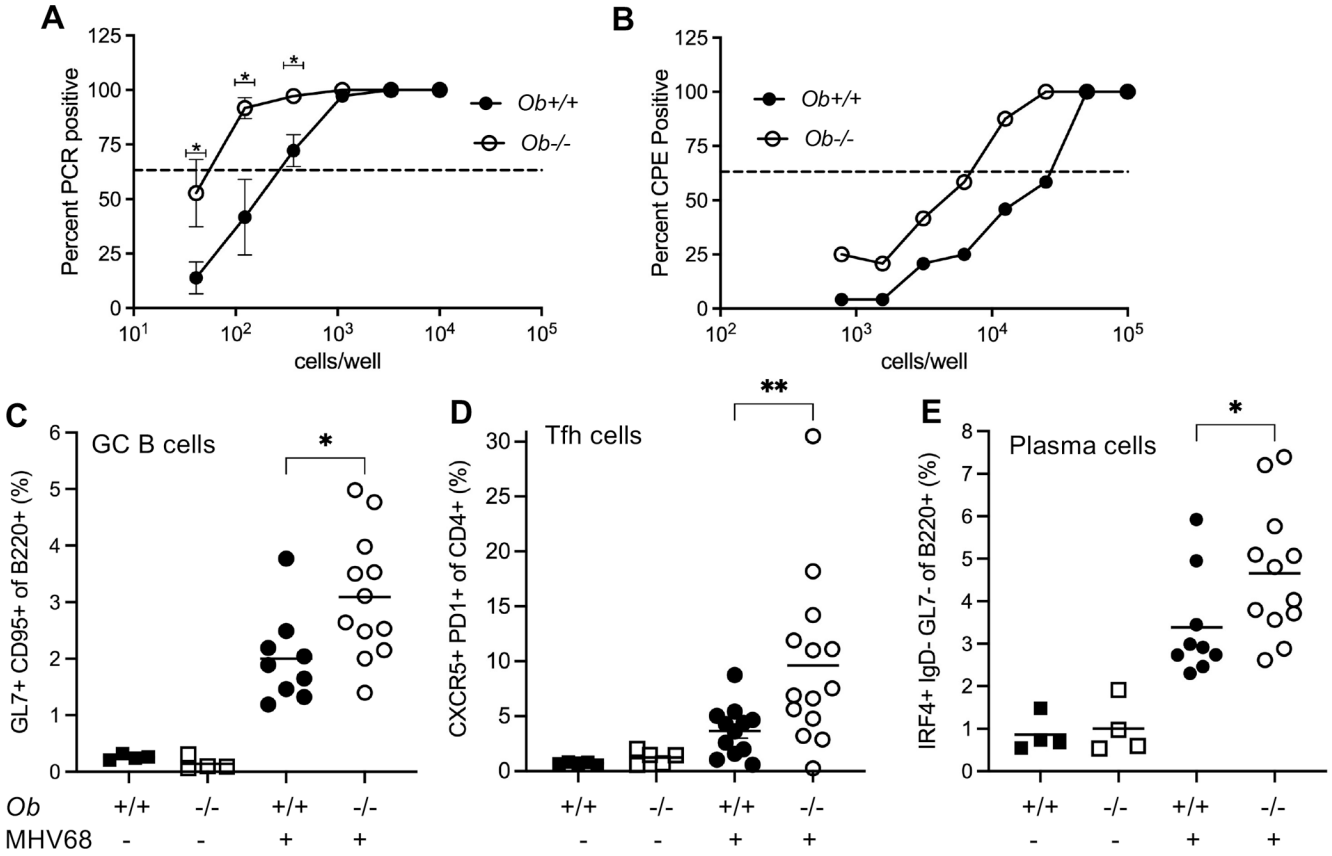

Figure 5. H2-O expression restricts establishment of viral latency and MHV68-driven germinal center responses.

Six to 7-week-old B6J.$Ob^{+/+}$ and $Ob^{-/-}$ mice were intranasally inoculated with 10^3 PFUs of MHV68. Splenocytes were collected and analyzed at 16 days post infection. **A**, enumeration of latently infected splenocytes (pooled samples within each experimental group, 3–5 mice/group) by limiting dilution analyses. **B**, viral reactivation *ex vivo*. In the limiting dilution assays the dotted line is drawn at 62.5% and the X-coordinate of intersection of this line with the sigmoid graph represents an inverse frequency of positive events. Data in **A** is pooled from 3 independent experiments, data in **B** is representative of two independent experiments. **C-E**: abundance of indicated immune populations in splenocytes from mock- or MHV68-infected mice was determined by flow cytometry using indicated markers. Each symbol represents an individual animal. Gating strategies are shown in Figure S3. Significance was calculated using unpaired *t* tests. *=p≤ 0.05, **=p ≤0.01. Four uninfected $Ob^{+/+}$, 4 uninfected $Ob^{-/-}$, 12 infected $Ob^{+/+}$ and 14 infected $Ob{-/-}$ mice were used.